

## BASIC RESEARCH

# *In vitro* comparative study of white and dark polycaprolactone trifumarate *in situ* cross-linkable scaffolds seeded with rat bone marrow stromal cells

Kama Bistari Muhammad,<sup>1</sup> Wan Abu Bakar Wan Abas,<sup>1</sup> Kah Hwi Kim,<sup>11</sup> Belinda Pinguan-Murphy,<sup>1</sup> Norita Mohd Zain,<sup>1</sup> Haris Akram<sup>1</sup>

<sup>1</sup>University of Malaya, Faculty of Engineering, Department of Biomedical Engineering, Kuala Lumpur, Malaysia. <sup>11</sup>University of Malaya, Faculty of Medicine, Department of Physiology, Kuala Lumpur, Malaysia.

**OBJECTIVE:** Dark poly(caprolactone) trifumarate is a successful candidate for use as a bone tissue engineering scaffold. Recently, a white polymeric scaffold was developed that shows a shorter synthesis time and is more convenient for tissue-staining work. This is an *in vitro* comparative study of both the white and dark scaffolds.

**METHODS:** Both white and dark poly(caprolactone) trifumarate macromers were characterized via Fourier transform infrared spectroscopy before being chemically cross-linked and molded into disc-shaped scaffolds. Biodegradability was assessed by percentage weight loss on days 7, 14, 28, 42 and 56 (n=5) after immersion in 10% serum-supplemented medium or distilled water. Static cell seeding was employed in which isolated and characterized rat bone marrow stromal cells were seeded directly onto the scaffold surface. Seeded scaffolds were subjected to a series of biochemical assays and scanning electron microscopy at specified time intervals for up to 28 days of incubation.

**RESULTS:** The degradation of the white scaffold was significantly lower compared with the dark scaffold but was within the acceptable time range for bone-healing processes. The deoxyribonucleic acid and collagen contents increased up to day 28 with no significant difference between the two scaffolds, but the glycosaminoglycan content was slightly higher in the white scaffold throughout 14 days of incubation. Scanning electron microscopy at days 1 and 14 revealed cellular growth and attachment.

**CONCLUSIONS:** There was no cell growth advantage between the two forms, but the white scaffold had a slower biodegradability rate, suggesting that the newly synthesized poly(caprolactone) trifumarate is more suitable for use as a bone tissue engineering scaffold.

**KEYWORDS:** Bone Tissue Engineering; Polycaprolactone; Biodegradable Polymer; Bone Marrow; Mesenchymal Stem Cells.

Muhammad KB, Abas WA, Kim KH, Pinguan-Murphy B, Zain NM, Akram H. *In vitro* comparative study of white and dark polycaprolactone trifumarate *in situ* cross-linkable scaffolds seeded with rat bone marrow stromal cells. Clinics. 2012;67(6):629-637.

Received for publication on February 15, 2012; First review completed on February 21, 2012; Accepted for publication February 27, 2012

E-mail: bistari@um.edu.my / bistari@gmail.com

Tel.: 603 7967-7616

## INTRODUCTION

With over 2 million patients suffering from skeletal defects each year (1,2), the need for bone tissue engineering is apparent. The most popular approach used in bone tissue engineering is seeding stem cells onto a biodegradable porous scaffold and expanding them *in vitro* prior to implantation. However, this technique may require open surgery or dissection that prolongs recovery time, is traumatic to the connective tissue, and leads to scarring due to a large incision (3-5).

The increasing popularity of arthroscopic procedures in orthopedics has led to the development of *in situ* cross-linkable materials that are easily implanted *in vivo*. The main advantages of this procedure are that it is less invasive and better suited for treating irregularly shaped osseous defects (5-8). The most commonly used injectable bone cement is poly(methyl methacrylate) (PMMA). The injected bone cement, however, is permanent at the site, which may pose a serious risk of infection in addition to bone resorption due to stress shielding (9,10). Injectable *in situ* calcium phosphate, such as calcium-deficient hydroxyapatite and its blends, has been developed and causes no extended inflammatory reaction (11,12). However, its low tensile and shear strength limits its function, making it subject to fracture (13).

An *in situ* assembling monomer for repairing a bone defect must be not only biocompatible but also biodegradable. This characteristic can be achieved by incorporating

**Copyright** © 2012 CLINICS – This is an Open Access article distributed under the terms of the Creative Commons Attribution Non-Commercial License (<http://creativecommons.org/licenses/by-nc/3.0/>) which permits unrestricted non-commercial use, distribution, and reproduction in any medium, provided the original work is properly cited.

No potential conflict of interest was reported.

enriched double-bond fumarate compounds inside a polyester, such as the photo-cross-linkable poly(anhydrides) (14), or a chemically cross-linkable compound, such as poly(propylene) fumarate (15) or poly(ethylene glycol) fumarate (16). These modified polymers degrade via hydrolysis, and their degradation and mechanical properties can be controlled by manipulating the amount of the cross-linking agent, e.g., methyl methacrylate (MMA) or N-vinyl-pyrrolidone (NVP) monomer (17,18). However, cross-linking agents are toxic and can cause undesirable effects on tissue cells (19).

A self-cross-linkable degradable material known as poly( $\epsilon$ -caprolactone) trifumarate (PCLTF) was synthesized by copolymerization of fumaryl chloride (FCl) and poly( $\epsilon$ -caprolactone) triol (PCL-triol) (20). PCL, which is used as a resorbable suture, has excellent biodegradability and biocompatibility. Its macromer has a flexible backbone, allowing self-cross-linking without the use of any cross-linking agent (19). The main drawback of PCLTF was its dark brownish color due to the use of triethylamine as its catalyst in mixing PCL and FCl to synthesize the PCLTF macromer. This unappealing appearance is not commercially friendly and causes difficulties for tissue-staining work. A whiter form of PCLTF was synthesized by replacing triethylamine with potassium carbonate ( $K_2CO_3$ ) as the proton scavenger (21). This new synthetic route not only yields a more appealing appearance but is also more convenient and less time consuming to synthesize. However, use of the improved method is futile if the modified form does not promote cell growth.

Although extensive *in vivo* and *in vitro* cell studies have been successfully carried out to validate the biocompatibility of dark PCLTF (19,20), none have been performed on white PCLTF. This study is a comparative study on scaffolds synthesized from both types of PCLTF that examines the biodegradability, the biochemical evaluations and preliminary observations of the cell attachment to both PCLTF scaffolds using rat bone marrow stromal cells (BMSCs) as a cell source. Rats were chosen because they are widely used for standard *in vitro* testing, and osteogenesis from rat BMSCs is widely established.

## MATERIALS AND METHODS

### Synthesis and purification of the PCLTF macromer

White PCLTF was synthesized by adopting the method of Wang et al. (21), which was modified to use PCL-triol ( $M_w=900$ ) instead of PCL-diol and a molar ratio of 0.9:1:1.2 instead of 0.9:1:1.5 for the FCl, PCL-triol and  $K_2CO_3$  mixture. PCL-triol was dissolved in methylene chloride in a three-necked flask before powdered  $K_2CO_3$  was added. The mixture was stirred with an overhead mechanical stirrer while FCl was added dropwise. The polymerization process was maintained at room temperature under a nitrogen atmosphere for the next 12 hours to form a white macromer.

Dark PCLTF was synthesized similar to the method described above but with FCl, PCL-triol and triethylamine at a molar ratio of 1.1:1:2.5 (22). Furthermore, triethylamine in liquid form was added dropwise concurrently with FCl. This mixture was stirred in an ice bath for the first 2 hours. Nitrogen gas was then extracted, and stirring continued at room temperature for a total reaction time of 48 hours to form a dark macromer.

At the end of the reaction time, macromers were transferred to centrifuge tubes and centrifuged for 15 minutes at 4,000 RPM until the precipitates (unreacted catalysts and triethylammonium chloride or potassium chloride) were completely removed. The supernatant was further purified by adding it dropwise to petroleum ether to extract the polymer, and it was rotary-evaporated to yield a waxlike structure.

### Characterization of polymers by FT-IR spectroscopy

Fourier transform infrared (FT-IR) spectroscopy was employed to confirm the formation of the PCLTF macromer by identifying double-bond groups in the PCL backbones. The FT-IR spectra were obtained on a Spectrum RX1 (Perkin Elmer Sdn Bhd, Petaling Jaya, Selangor, Malaysia) spectrometer using a sodium chloride plate as the sample holder.

### Fabrication of porous scaffolds

The PCLTF scaffold was fabricated by chemical self-cross-linking using benzoyl peroxide (BP) and *N*-dimethyl-*o*-toluidine (DMT) as the cross-linking initiator and accelerator, respectively, with sodium chloride (NaCl) salt particles sieved at 200–300  $\mu$ m as the porogen. A ratio of 1:1 PCLTF macromer to NaCl was mixed together before cross-linking was initiated. For each gram of macromer, 12.5  $\mu$ g BP dissolved in 170  $\mu$ l NVP and 10  $\mu$ l DMT were added and mixed together. NVP (less than 2% by weight of the macromer) was used as a BP solvent, not as a cross-linking agent. A total of 3 g of the cross-linked mixture was evenly spread in a  $\varnothing$  3.5 cm NUNC Hydrocell<sup>TM</sup> Petri dish and allowed to gel at 60°C in a convection oven for 1 hour. After cross-linking, the ~1 mm-thick mold was cooled to ambient temperature before salt leaching. The scaffold sheets were gently removed from the Petri dish and soaked in distilled water for 4 days, and the water was changed every 12 hours. The sheets were freeze-dried overnight before they were cut into  $\varnothing$  6 mm disc-shaped scaffolds.

### Biodegradability test

The mass of each white and dark PCLTF scaffold was determined as  $DW_i$  before they were immersed in an excess of either Dulbecco's modified Eagle's medium (DMEM) supplemented with 10% bovine serum or distilled water, capped in vials, and incubated in a shaking bath at 37°C and 70 RPM. The pH was held constant at 7.4 by changing the solution every 24 hours during the incubation period of 7, 14, 28, 42, and 56 days ( $n=5$  for each group). The scaffolds were then removed from the vials and dabbed with a lint-free tissue to remove excess fluid before subsequent overnight drying at 60°C. The dried weight was measured as  $DW_f$ . The weight loss at each time point was determined by the following equation:

$$\frac{DW_i - DW_f}{DW_i} \times 100\%$$

The test was repeated on commercial PCL scaffolds (Biotek), which acted as a control. The mean values of each sample group and control were compared using ANOVA (two factor with replication) and Student's *t*-test for each point of incubation against  $\alpha=0.05$ .

### Isolation and cell culture

BMSCs were obtained from young adult 150-200 g male Sprague Dawley rats using the method of Maniatopoulos et al. (23), and the isolation protocols were approved by the Animal Ethics Committee [Ethics Reference No: BM/10/11/2008/KBM(R)], Faculty of Medicine, University of Malaya. The cell suspension was plated in T-75 flasks in primary media containing DMEM/F12 supplemented with Glutamax (Gibco), HEPES buffer (Gibco), 10% Fetal Bovine Serum (FBS) (Gibco), and 1% antibiotic/antimycotic solution (Gibco) and incubated in 95% relative humidity and 5% CO<sub>2</sub> at 37°C. The medium was changed every 48 hours until cells reached 75% confluence, and cells between passages 1 and 2 were used for seeding the scaffolds.

### Cell characterization

A direct live staining method was employed on a single-cell suspension with mouse anti-rat CD31-PE, CD45-FITC, and CD90.Thy1-PerCP monoclonal antibodies (BD Biosciences) with flow cytometry analysis. Corresponding isotype and positive control experiments were performed for each antibody. The samples were analyzed with a FACSCanto, and data were acquired at 10,000 to 50,000 events using FACSDiva software. Proper gating and compensation were carried out to exclude debris and to correct the spectral spillover from the combined fluorochromes.

The differentiation ability of the isolated cells was evaluated by culturing the remaining cells in osteogenic medium before seeding onto the PCLTF scaffolds. The osteogenic medium consisted of DMEM/F12 supplemented with 10% FBS, 0.1 μM dexamethasone, 10 mM β-glycerol phosphate, and 0.2 mM ascorbic acid. A cell suspension was incubated and stained with Alizarin Red S to determine the osteogenesis of the isolated cells.

### Cell Seeding

Standard static seeding was employed on the ø 6×1 mm PCLTF porous scaffold discs. The discs were first soaked in 70% ethanol overnight, followed by prewetting with sterile primary medium for 2 hours. Trypsinized cells were centrifuged and resuspended in primary medium before being diluted to 2×10<sup>5</sup> cells/ml. Aliquots of 20 μl of cell suspension containing ~40,000 cells were pipetted onto the top of prewetted PCLTF discs and left in the incubator for 2 hours to facilitate cell attachment. The seeded PCLTF porous discs were transferred to a 24-well plate, and 1 ml of primary media was gently added to each well. The plate was incubated in 5% CO<sub>2</sub> at 37°C with 95% relative humidity, and the medium was changed every 2 days.

### Scanning Electron Microscopy (SEM)

Samples of unseeded and seeded (day 1 and 14) white and dark PCLTF scaffolds were processed for SEM. The samples were fixed in 4% glutaraldehyde followed by 1% osmium tetroxide and dehydrated with an ethanol series to 100% before being gold coated. The images of BMSC attachments and cell interactions between each group were compared.

### Biochemical Assays

Seeded white and dark PCLTF scaffolds (n=8) were removed from tissue plates at days 3, 7, 14, 21, and 28 after

incubation, digested with papain enzyme buffered at pH 6.5 and incubated at 60°C overnight. Postdigestion samples were centrifuged to remove debris before being subjected to biochemical assays. The Hoechst 33258 assay was carried out for DNA quantification using filtered calf thymus as the standard DNA (24). Proteoglycans/glycosaminoglycans (GAG) and collagen were quantified with BLYSCAN and SIRCOL assay kits (Biocolor). Unseeded scaffolds were sampled as the zero reference for each assay. The absorbance was measured using a FluoStar Optima, and the percentage increase in the mean values for each time point was determined by the following equation:

$$\frac{A_d - A_o}{A_o} \times 100\%$$

where A<sub>d</sub>=mean absorbance at day d and A<sub>o</sub>=mean absorbance at day 0 after seeding. The percentage increase in the mean absorbance between white and dark PCLTF scaffolds was compared for each assay using ANOVA at α=0.05.

## RESULTS AND DISCUSSION

### Synthesis and purification of the PCLTF macromer

The synthesized PCLTF macromers are both unsaturated, highly branching polyesters containing double bonds originating from FCI integrated into the poly(caprolactone) backbone. The only difference is that the use of triethylamine has resulted in an opaque dark color, while the modified method of using K<sub>2</sub>CO<sub>3</sub> has yielded a translucent white color for the final product (Figures 1A and B). This change in appearance is advantageous for cell studies involving staining and observation under a light microscope.

The synthesis process was considered complete when the homogeneous texture, color, and viscosity remained unchanged for 24 hours. The use of K<sub>2</sub>CO<sub>3</sub> has shortened the reaction time from 48 to 12 hours because the polycondensation between PCL and FCI has yielded relatively higher-molecular-weight copolymers compared with the use of triethylamine (21). Furthermore, polycondensation with K<sub>2</sub>CO<sub>3</sub> as the proton scavenger is more stable than triethylamine. This stability allows the improved method to be carried out at room temperature without degrading the macromers in contrast to the conventional method, which had to be controlled in an ice bath to limit the temperature increase of the volatile exothermic reaction (19). This higher temperature increases the overall rate of the reaction.

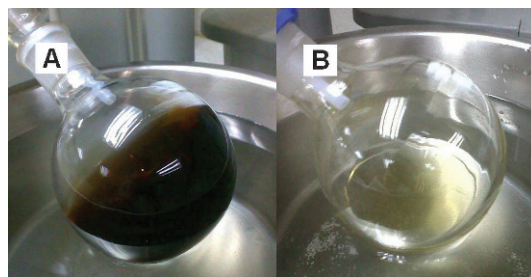


**Figure 1** - The dark PCLTF macromer (A) was dark brownish and opaque, whereas the white PCLTF macromer (B) was light yellow and translucent.

The greater degree of reaction between PCL and FCl has yielded a thicker end product. Thus, the ratio of FCl to PCL triol was reduced from 1.1:1 to 0.9:1 to avoid macromere solidification from intense polycondensation.

$K_2CO_3$  has also neutralized active chlorine anions released from FCl to prevent the formation of unpleasant byproduct HCl gas (25). This neutralization was shown by the absence of white fumes, which were visible during dark PCLTF macromere synthesis.

### Characterization of the PCLTF macromer

The incorporation of double bonds originating from FCl into the poly(caprolactone) backbone was confirmed by the presence of C=C and =C-H stretches in the PCLTF (both white and dark) FT-IR spectra, which occur at  $1,600-1,660\text{ cm}^{-1}$  and  $3,010-3,095\text{ cm}^{-1}$ , respectively (26). These two stretches were absent in the PCL-triol spectrum (Figure 2). Furthermore, the hydroxyl groups (-OH), which are visible in PCL-triol at  $3,520\text{ cm}^{-1}$ , have diminished in both white and dark PCLTF due to deprotonation from FCl (Figure 2).

### Fabrication of a porous PCLTF scaffold

Significant cross-linking of the PCLTF macromer was achieved in 15 to 30 minutes. Without DMT, the cross-linking reaction was only completed after overnight incubation. This slower reaction reflected the role of DMT in accelerating the cross-linking process. Through salt particle leaching, scaffolds with interconnected pores were obtained. NUNC Hydrocell Petri dish surfaces were designed for low attachment. An approximately 1 mm-thick round sheet was formed using the Hydrocell dish and was easily removed by soaking in distilled water. Using a  $\varnothing$  6 mm hollow cylindrical tool, approximately 18 to 20 discs were cut and produced from the round sheet. When examined under a light microscope, the small discs had a

translucent gel-like appearance with a rough and porous structure.

### Biodegradability test

Dark PCLTF scaffold degrades up to 30% by 8 weeks of incubation, which is significantly higher than the white PCLTF scaffold (ANOVA:  $p < 0.0001$ ) and standard PCL scaffold (ANOVA:  $p < 1 \times 10^{-40}$ ), which degrade less than 11% and 5%, respectively (Figure 3). PCL shows the least degradation compared with PCLTF groups due to the absence of NVP, which is strongly hygroscopic and miscible with water (27). It is believed that the hygroscopic property of NVP, which tends to absorb moisture or water from the external medium, within PCLTF scaffolds softened the PCLTF scaffolds and rendered them more susceptible to biodegradation.

Additionally, it was anticipated that the dark PCLTF scaffold would have a higher degradation rate than the white PCLTF scaffold. As mentioned earlier in *Synthesis and purification of the PCLTF macromer*, white PCLTF has a higher degree of reaction with FCl; thus, more -OH groups were reduced to C=C bonds. This result was supported by a smaller -OH peak and higher C=C and =C-H peaks in white PCLTF spectra compared with dark PCLTF spectra, as shown in Figure 2. This highly cross-linked network structure and fewer hydroxyl groups reduce water absorption, which decreases white PCLTF scaffold degradation. Hoffman (28) determined that the water degradation of scaffolds began when water molecules entered the matrix and hydrated the most polar hydrophilic groups, i.e., -OH groups, thus exposing hydrophobic groups to water molecules. The hydrated network would incorporate additional water via the osmotic driving force of the network chains toward infinite dilution. However, this additional covalent force from the cross-linked network opposes the swelling, forming a retraction force. As a result, the degradation rate is reduced.

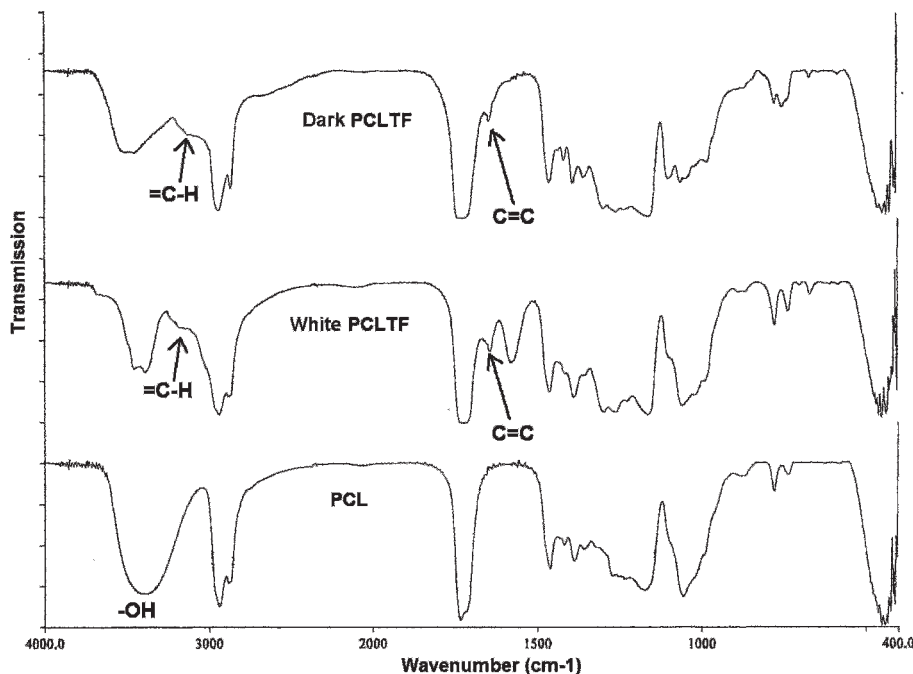
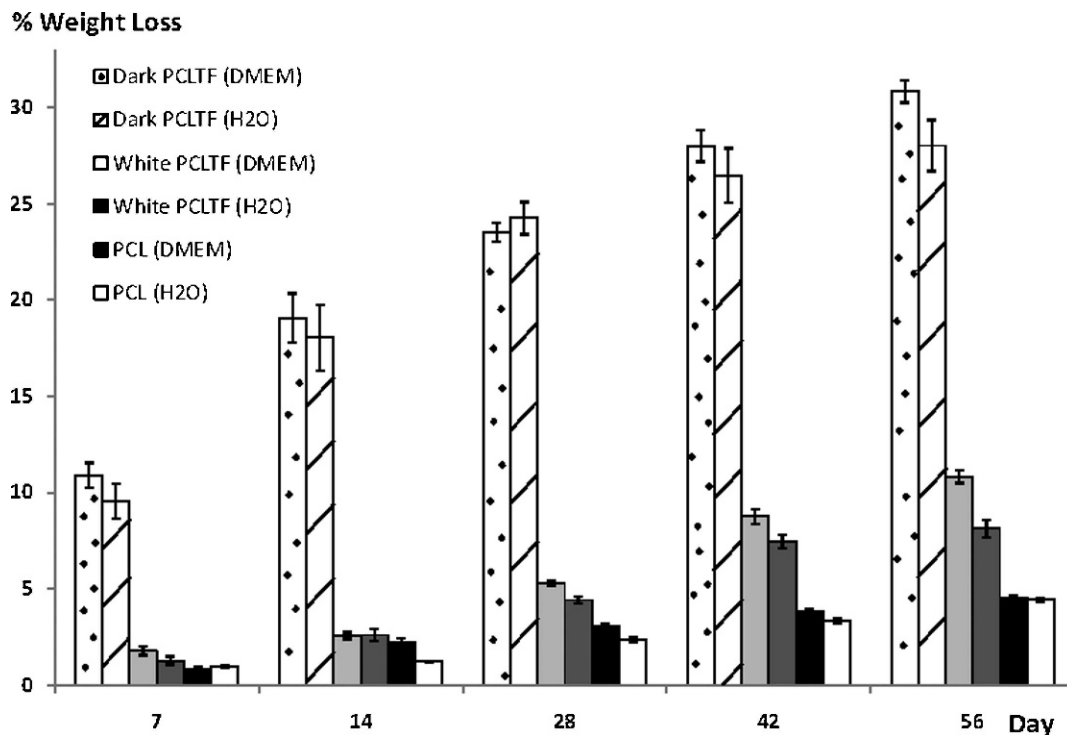


Figure 2 - FT-IR spectra of dark PCLTF, white PCLTF and PCL.





**Figure 3** - Percentage weight loss over time of dark PCLTF, white PCLTF, and PCL scaffolds immersed in DMEM or distilled water, with 95% confidence intervals. Weight loss was measured in five independently incubated samples. Dark PCLTF demonstrated the highest degradation, followed by white PCLTF and PCL ( $30.86 \pm 1.15\%$ ,  $10.83 \pm 0.66\%$ , and  $4.55 \pm 0.26\%$ , respectively, by day 56, immersed in DMEM).

Bone injury may recover to 80% of normal within 8-14 weeks, but the complete bone-healing process takes between 18 and 20 months (29,30). Extrapolating the percentage weight loss over time (figure not shown) has shown that the complete degradation of dark PCLTF, white PCLTF, and standard PCL scaffold was estimated at 18, 22, and 46 months, respectively. This result indicates that the degradation of the white PCLTF scaffold falls within the most acceptable range; it is able to provide structural support throughout the healing time and fully degrades within 2 to 4 months after the end of the healing process.

Except for PCL, the degradation kinetics showed a trend of becoming slower with increased incubation time. This result reflected the surface area to volume ratio effect, which decreases as the scaffold degrades, thus decreasing interactions with the incubation medium, such as water or DMEM.

DMEM and distilled water were used to study the type of degradation in the PCLTF scaffolds by comparing the combined hydrolysis and tricarboxylic acid metabolism from DMEM immersion with the exclusive hydrolytic effect from water immersion. Figure 3 shows that the weight loss was slightly higher in DMEM. ANOVA showed a significant difference between the two media ( $p < 0.0002$ ). However, individual Student's t-test analyses showed no significant differences in weight loss at several time points between PCL and white PCLTF and at all of the time points with dark PCLTF ( $p$  ranging from 0.1 to 0.9). Therefore, the effect of the medium on degradation was inconclusive.

In interpreting these results, it is important to note that the use of immersion tests alone may lead to an underestimation of the final *in vivo* degradation rate (31).

### Isolation and Cell Culture

DMEM/F12 with Glutamax was chosen as the primary medium after a series of media trials showed that DMEM/F12 produces the fastest growth of BMSCs, with 80% confluence as early as 4 days after bone marrow isolation. Suspended cells and unwanted residues floated away, while plastic adherent spindle-shaped cells attached to and proliferated on the flask surface. The BMSCs had apparent nuclei, were fibroblastic in shape, and showed quick growth, which allowed healthy cell-to-cell interactions.

### Cell Characterization

Flow cytometry analysis (Figures 4A, B and C) has shown that the majority of the isolated cell populations are CD31-/CD45-/CD90.Thy1+ (41.1%) and CD31-/CD45+/CD90.Thy1- (48.3%). A total of 41.1% of the population (Q1 in Figure 4B) was phenotypically characteristic of mesenchymal stem cells (MSC) and was negative for endothelial marker CD31 and hematopoietic marker CD45 but positive for CD90.Thy1, which is a general marker for three types of cells: endothelial cells, hematopoietic stem cells and MSCs (32). Because CD31 was negative, it is safe to conclude that the expression of CD90.Thy1 represented MSCs alone. A total of 48.3% of the population (Q4 in Figure 4B) was fibrocytes (33,34), which are mesenchymal precursor cells that can differentiate into myofibroblasts and fibroblasts. The presence of fibrocytes agreed with the hypothesis that plated cells may differentiate into the fibroblastic lineage by default. Because the flow cytometry samples were tested after the first passage in T-75 culture flasks, it is possible that some of the MSCs had differentiated into fibrocytes. More study is

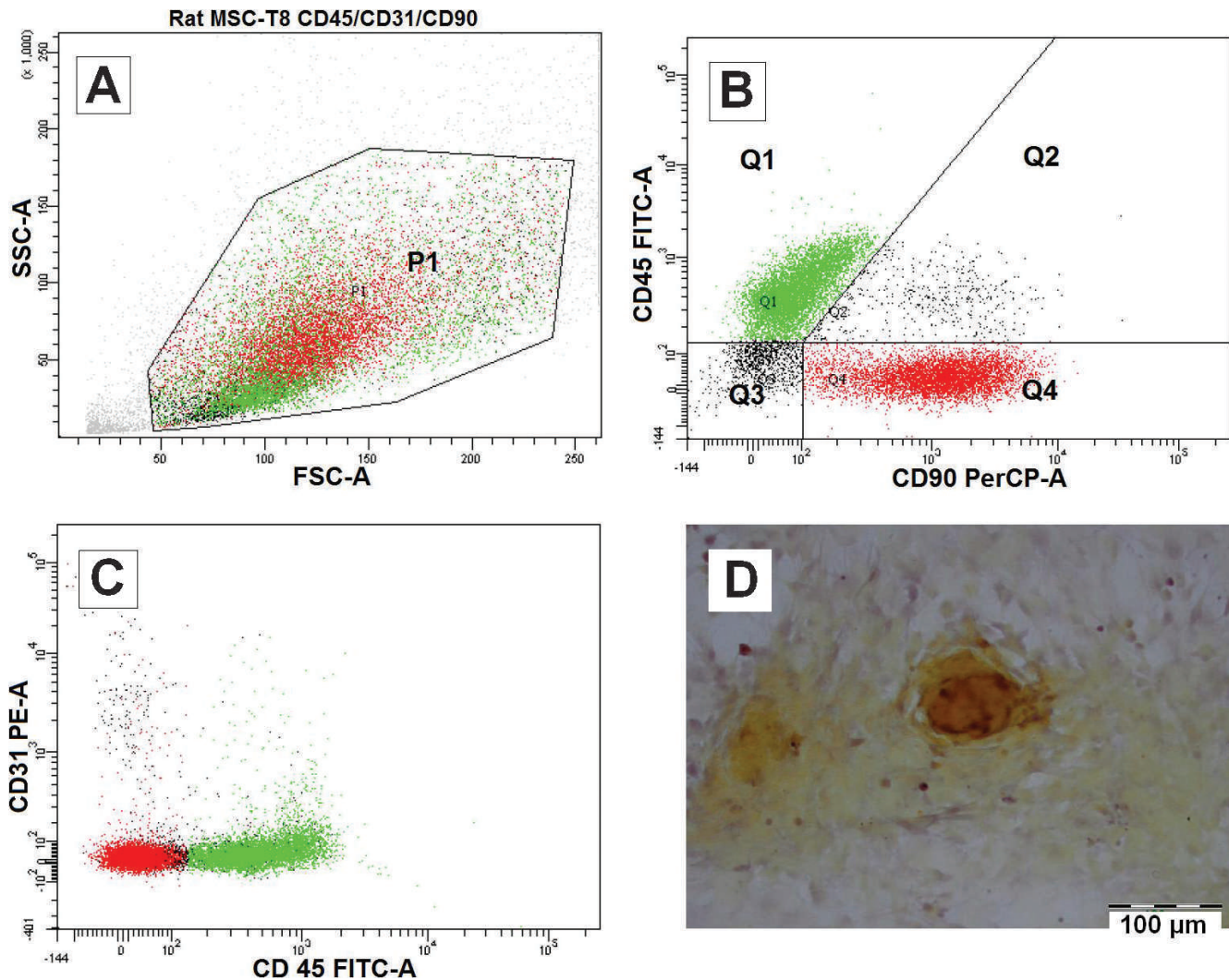


**Figure 4 -** Characterization of isolated cells from rat bone marrow after passage 1. Cells were analyzed with BD FACSDiva software (A, B and C). The P1 population (A) was divided into four quartets, of which 48.3% were Q1:CD31-/CD45+/CD90- and 41.1% were Q4:CD31-/CD45-/CD90+, which are indicated in green and red, respectively (B and C). Alizarin Red S staining of separate isolated cells has demonstrated the active deposition of calcified minerals after 14 days of osteogenic medium induction (D).

required to obtain evidence of this hypothesis, and it remains unclear whether the fibrocytes were indeed derived from the MSCs or whether they preexisted along with MSCs in the bone marrow.

Although the majority of the sample population was fibrocytes, the differentiation ability of the osteoblastic lineage was unaffected. Alizarin Red staining, as shown in Figure 4D, has confirmed the presence of osteoblasts after 14 days of induction in osteogenic medium. This result suggested that the fibrocytes may have dedifferentiated into stem cells and responded well to the osteogenic induction, which supports the hypothesis of the reversible behavior of fibrocytes (35,36).

### Cell Seeding

Static seeding was an appropriate method to study the two fabricated PCLTF scaffolds *in vitro*. Both of the seeded groups have generated significant cell growth at day 7, and after 28 days, a significant cell layer and mineralization covering the entire outermost surface of scaffolds was

observed. This preliminary finding showed a successful *in vitro* study of the improved white PCLTF scaffold.

Cell growth has led to a change in the dark PCLTF scaffold's color from dark brown to yellow-whitish; likewise, white PCLTF was changed from white to light yellowish. This change could be due to the mineralization of the structure surface, which dominates the overall color of the construct.

No cells were found on the well surface, indicating efficient seeding.

### Scanning Electron Microscopy (SEM)

The interaction of BMSCs with both PCLTF scaffolds at days 1 and 14 was qualitatively characterized using SEM. The interaction test shows no advantage between white and dark PCLTF scaffolds at these time points. The unseeded scaffolds (both white and dark) have interconnected micropores, as shown in Figures 5A and 5B. The seeded BMSCs attached firmly to the scaffold surface by day 1 after incubation (Figures 5C and D). By day 14 after incubation, a



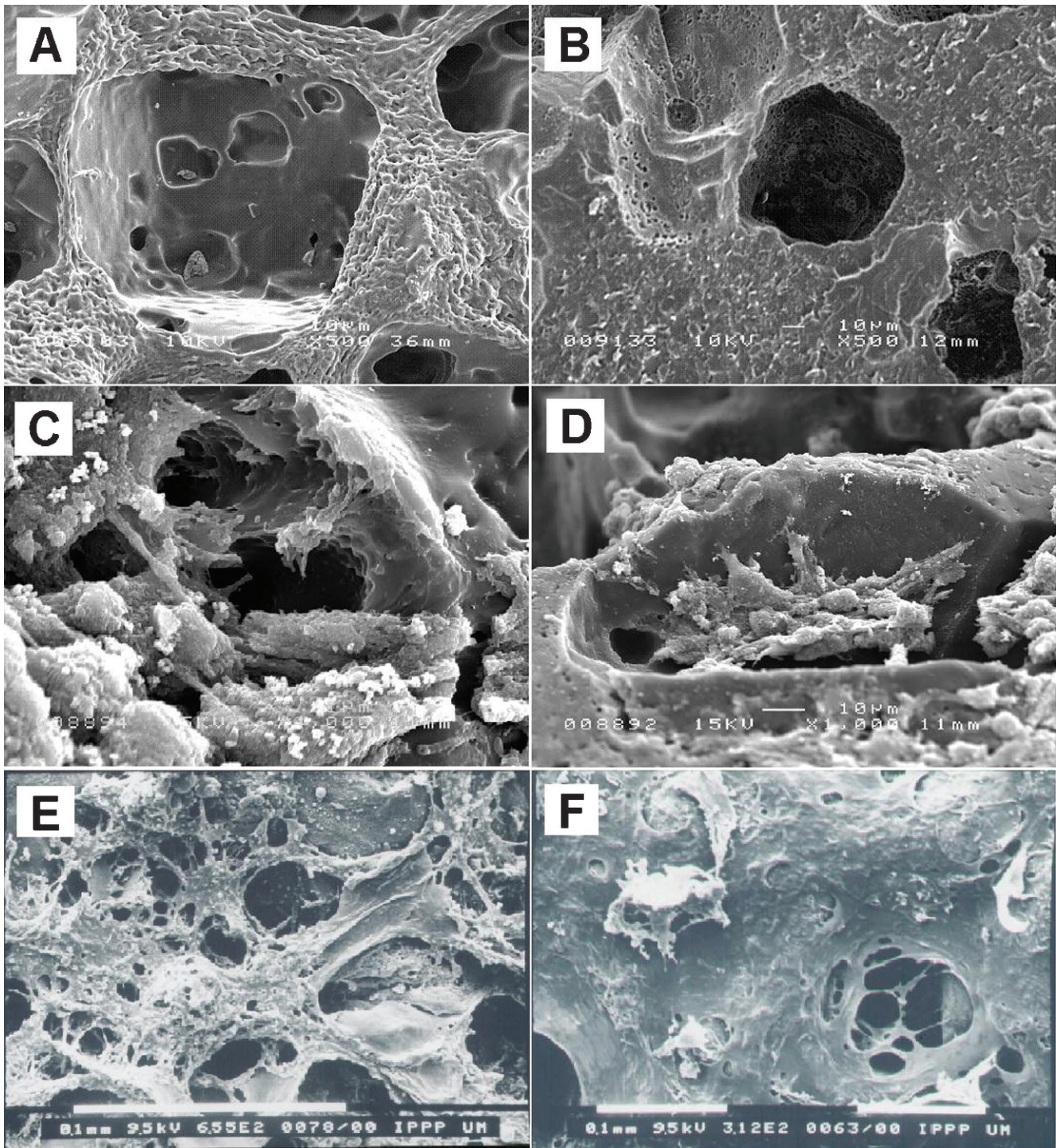


**Figure 5** - SEM analysis of unseeded (A and B), 1 day after MSC seeding (C and D) and 14 days after MSC seeding (E and F) white and dark PCLTF scaffolds.

well-formed cellular layer with active extracellular matrix secretion was visible (Figures 5E and F).

#### Biochemical Assays

Figures 6A, B and C show significant increases in all of the assays over time, which plateaued by day 28 (except for GAG because the GAG increase was only quantified until the 14<sup>th</sup> day). There was no significant difference between white and dark PCLTF in terms of DNA or collagen increase

(ANOVA:  $p=0.212$  and  $0.179$ , respectively), but there was a significant difference in GAG (ANOVA:  $p<1\times 10^{-4}$ ). Figure 6B shows that the percentage increase in GAG was slightly higher in white PCLTF throughout 14 days of incubation.

There was no advantage in cell growth or extracellular matrix deposition for either of the two PCLTF scaffolds, but the white scaffold had a slower biodegradability rate, which remained within the acceptable range and was associated



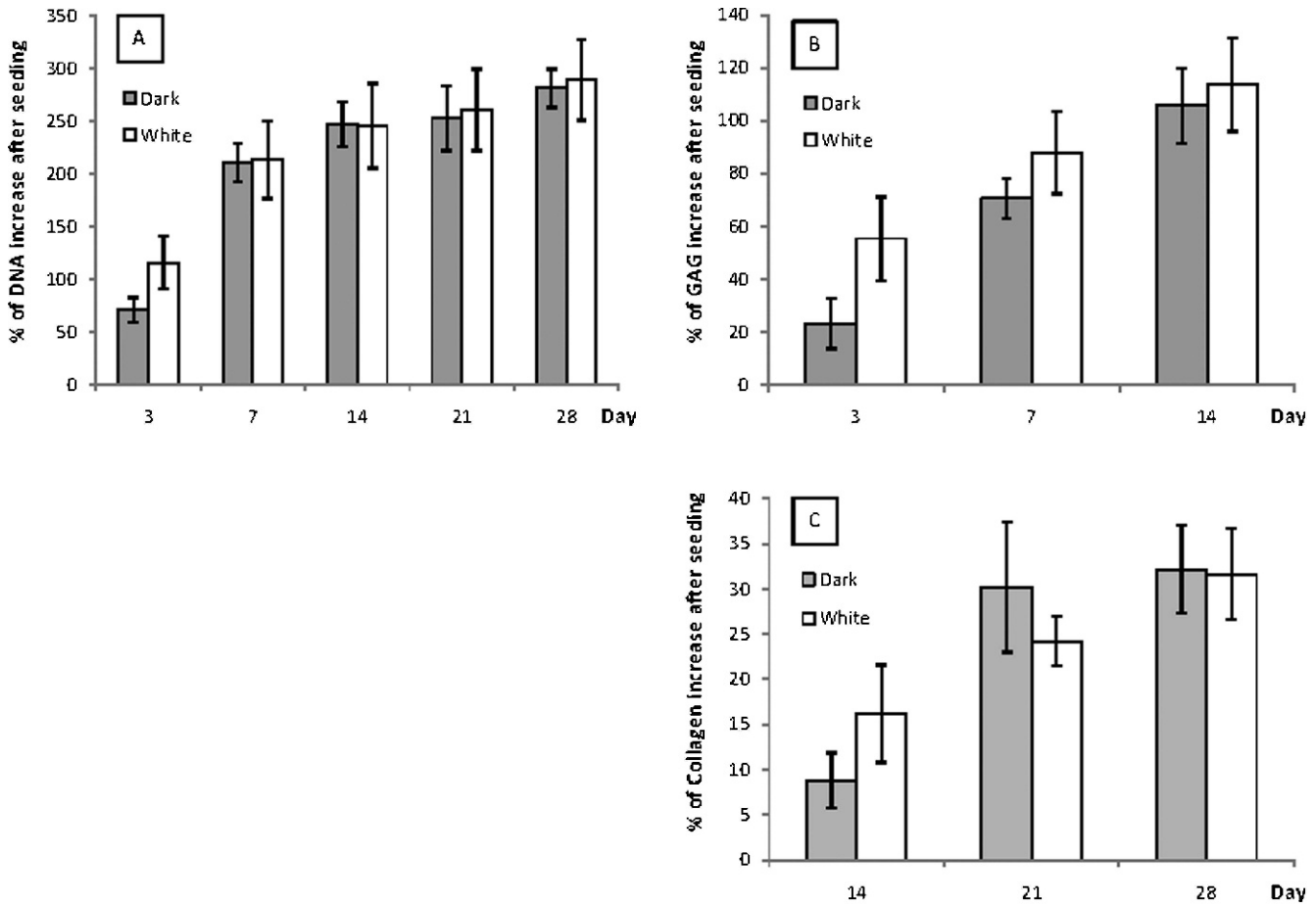


Figure 6 - Percentage of DNA (A), GAG (B) and collagen (C) after seeding, with 95% confidence intervals.

with a slight increase in GAG content. These data suggest that the improved synthesis method to form white PCLTF does not compromise its biocompatibility or discourage cell growth. Therefore, white PCLTF is suitable for use as a bone tissue engineering scaffold and may replace the conventional dark PCLTF.

### ACKNOWLEDGMENTS

We sincerely thank Mr. Mohd Fairuz Zainal Abidin from the Department of Chemistry and Mr. Chew Poh Wei for their technical assistance. This project was funded by the University of Malaya under the University of Malaya Research Grant (Project no.: RG043/09AET) and Postgraduate Research Grant (Project no.: PS391/2010A).

### AUTHOR CONTRIBUTIONS

Muhammad KB was the main researcher of the entire project. Wan Abas WA provided advice and funding for the project. Kim KH provided advice, access to animals and advice on scaffold synthesis. Murphy B provided access to and advice on biochemical assays and edited the manuscript before submission. Zain NM provided technical assistance and advice on the biodegradability study. Akram H provided technical assistance on the isolation and culture of bone marrow stromal cells from rat.

### REFERENCES

1. Einhorn TA. Orthopedic gene therapy: Building bones. *Gene Therapy*. 2003;10(7):529, <http://dx.doi.org/10.1038/sj.gt.3302000>.
2. Langer R, Vacanti J. Tissue engineering. *Science*. 1993;260(5110):920-6, <http://dx.doi.org/10.1126/science.8493529>.

3. Anseth KS, Shastri VR, Langer R. Photopolymerizable degradable polyanhydrides with osteocompatibility. *Nature Biotechnology*. 1999;17(2):156-9.
4. Yaszemski MJ, Payne RG, Hayes WC, Langer R, Mikos AG. In vitro degradation of a poly(propylene fumarate)-based composite material. *Biomaterials*. 1996;17(22):2127-30, [http://dx.doi.org/10.1016/0142-9612\(96\)00008-7](http://dx.doi.org/10.1016/0142-9612(96)00008-7).
5. Burdick JA, Philpott LM, Anseth KS. Synthesis and characterization of tetrafunctional lactic acid oligomers: A potential *in situ* forming degradable orthopaedic biomaterial. *Journal of Polymer Science Part A: Polymer Chemistry*. 2001;39(5):683-92, [http://dx.doi.org/10.1002/1099-0518\(20010301\)39:5<683::AID-POLA1040>3.0.CO;2-Z](http://dx.doi.org/10.1002/1099-0518(20010301)39:5<683::AID-POLA1040>3.0.CO;2-Z).
6. Fisher JP, Dean D, Mikos AG. Photocrosslinking characteristics and mechanical properties of diethyl fumarate/poly(propylene fumarate) biomaterials. *Biomaterials*. 2002;23(22):4333-43, [http://dx.doi.org/10.1016/S0142-9612\(02\)00178-3](http://dx.doi.org/10.1016/S0142-9612(02)00178-3).
7. Shin H, Jo S, Mikos AG. Biomimetic materials for tissue engineering. *Biomaterials*. 2003;24(24):4353-64, [http://dx.doi.org/10.1016/S0142-9612\(03\)00339-9](http://dx.doi.org/10.1016/S0142-9612(03)00339-9).
8. Shastri VP, Padera RF, Tarcha P, Langer R. A preliminary report on the biocompatibility of photopolymerizable semi-interpenetrating anhydride networks. *Biomaterials*. 2004;25(4):715-21, [http://dx.doi.org/10.1016/S0142-9612\(03\)00563-5](http://dx.doi.org/10.1016/S0142-9612(03)00563-5).
9. Peter SJ, Lu L, Kim DJ, Mikos AG. Marrow stromal osteoblast function on a poly(propylene fumarate)/[beta]-tricalcium phosphate biodegradable orthopaedic composite. *Biomaterials*. 2000;21(12):1207-13, [http://dx.doi.org/10.1016/S0142-9612\(99\)00254-9](http://dx.doi.org/10.1016/S0142-9612(99)00254-9).
10. Temenoff JS, Mikos AG. Injectable biodegradable materials for orthopedic tissue engineering. *Biomaterials*. 2000;21(23):2405-12, [http://dx.doi.org/10.1016/S0142-9612\(00\)00108-3](http://dx.doi.org/10.1016/S0142-9612(00)00108-3).
11. Kopylov P, Jonsson K, Thorngren KG, Aspenberg P. Injectable calcium phosphate in the treatment of distal radial fractures. *The Journal of Hand Surgery: Journal of the British Society for Surgery of the Hand*. 1996;21(6):768-71.
12. Knaack D, Goad MEP, Aiolo M, Rey C, Tofighi A, Chakravarthy P, et al. Resorbable calcium phosphate bone substitute. *Journal of Biomedical*



- Materials Research. 1998;43(4):399-409, [http://dx.doi.org/10.1002/\(SICI\)1097-4636\(199824\)43:4<399::AID-JBM7>3.0.CO;2-J](http://dx.doi.org/10.1002/(SICI)1097-4636(199824)43:4<399::AID-JBM7>3.0.CO;2-J).
13. Constantz B, Ison I, Fulmer M, Poser R, Smith S, VanWagoner M, et al. Skeletal repair by *in situ* formation of the mineral phase of bone. *Science*. 1995 March 24, 1995;267(5205):1796-9.
  14. Poshusta AK, Burdick JA, Mortisen DJ, Padera RF, Ruehlman D, Yaszemski MJ, et al. Histocompatibility of photocrosslinked polyamides: A novel *in situ* forming orthopaedic biomaterial. *Journal of Biomedical Materials Research Part A*. 2003;64A(1):62-9, <http://dx.doi.org/10.1002/jbm.a.10274>.
  15. Domb AJ, Manor N, Elmalak O. Biodegradable bone cement compositions based on acrylate and epoxide terminated poly(propylene fumarate) oligomers and calcium salt compositions. *Biomaterials*. 1996;17(4):411-7, [http://dx.doi.org/10.1016/0142-9612\(96\)89657-8](http://dx.doi.org/10.1016/0142-9612(96)89657-8).
  16. Jo S, Shin H, Shung AK, Fisher JP, Mikos AG. Synthesis and Characterization of Oligo(poly(ethylene glycol) fumarate) Macromer. *Macromolecules*. 2001;34(9):2839-44, <http://dx.doi.org/10.1021/ma001563y>.
  17. He S, Timmer MD, Yaszemski MJ, Yasko AW, Engel PS, Mikos AG. Synthesis of biodegradable poly(propylene fumarate) networks with poly(propylene fumarate)-diacrylate macromers as crosslinking agents and characterization of their degradation products. *Polymer*. 2001;42(3):1251-60, [http://dx.doi.org/10.1016/S0032-3861\(00\)00479-1](http://dx.doi.org/10.1016/S0032-3861(00)00479-1).
  18. Frazier DD, Lathi VK, Gerhart TN, Hayes WC. Ex vivo degradation of a poly(propylene glycol-fumarate) biodegradable particulate composite bone cement. *Journal of Biomedical Materials Research*. 1997;35(3):383-9, [http://dx.doi.org/10.1002/\(SICI\)1097-4636\(19970605\)35:3<383::AID-JBM12>3.0.CO;2-G](http://dx.doi.org/10.1002/(SICI)1097-4636(19970605)35:3<383::AID-JBM12>3.0.CO;2-G).
  19. Jabbari E, Wang S, Lu L, Gruetzmacher JA, Ameenuddin S, Hefferan TE, et al. Synthesis, Material Properties, and Biocompatibility of a Novel Self-Cross-Linkable Poly(caprolactone fumarate) as an Injectable Tissue Engineering Scaffold. *Biomacromolecules*. 2005;6(5):2503-11, <http://dx.doi.org/10.1021/bm050206y>.
  20. Chai YC, Abas WAB, Kim KH. Osteogenic expression of bone marrow stromal cells on PCLTF scaffold: In vitro study. *Asian Journal of Cell Biology*. 2006;1(1):40-7.
  21. Wang S, Lu L, Gruetzmacher JA, Currier BL, Yaszemski MJ. Synthesis and characterizations of biodegradable and crosslinkable poly([epsilon]-caprolactone fumarate), poly(ethylene glycol fumarate), and their amphiphilic copolymer. *Biomaterials*. 2006;27(6):832-41, <http://dx.doi.org/10.1016/j.biomaterials.2005.07.013>.
  22. Chai YC, Abas WAB, Kim KH. Development and characterisation of a novel poly(caprolactone-trifumarate) macromer as scaffold for bone tissue engineering. *International Federation Med Biol Eng Proceed* 2004. p.359-62.
  23. Maniopoulos C, Sodek J, Melcher AH. Bone formation in vitro by stromal cells obtained from bone marrow of young adult rats. *Cell and Tissue Research*. 1988;254(2):317-30.
  24. Strauss WM. Preparation of Genomic DNA from Mammalian Tissue: John Wiley & Sons, Inc.; 2001.
  25. Peter SJ, Suggs LJ, Yaszemski MJ, Engel PS, Mikos AG. Synthesis of Poly(propylene fumarate) by acrylation of propylene glycol in the presence of a proton scavenger. *Journal of Biomaterials Science, Polymer Edition*, 1999;10(3):363-73.
  26. Pavia DL, Lampman GM, Kriz GS. Introduction to Spectroscopy: A Guide for Students of Organic Chemistry. 3rd ed. Bellingham: Brooks/Cole; 2001.
  27. Ali G. Effects of Inorganic Salts on the Spectral Behavior of Poly(N-vinyl-2-pyrrolidone) in Aqueous Solutions. *Journal of Applied Polymer Science*. 1999;75(11):1434-39.
  28. Hoffman AS. Hydrogels for biomedical applications. *Advanced Drug Delivery Reviews*. 2002;43:3-12, [http://dx.doi.org/10.1016/S0169-409X\(01\)00239-3](http://dx.doi.org/10.1016/S0169-409X(01)00239-3).
  29. Ross MH, Romrell LJ, Kaye GI. *Histology: A Text and Atlas*. 3rd ed. USA: Williams & Wilkins; 1995.
  30. Ham AW, Harris WR. *The Biochemistry and Physiology of Bone*. 2nd ed. New York: Academic Press; 1971.
  31. Smith TH, Engels TAP, Söntjens SMH, Govaert LE. Time-dependent failure in load-bearing polymers: a potential hazard in structural applications of polylactides. *Journal of Materials Science: Materials in Medicine*. 2010;21(3):871-78, <http://dx.doi.org/10.1007/s10856-009-3921-z>.
  32. Jones EA, Kinsey SE, English A, Jones RA, Straszynski L, Meredith DM, et al. Isolation and characterization of bone marrow multipotential mesenchymal progenitor cells. *Arthritis & Rheumatism*. 2002;46(12):3349-60, <http://dx.doi.org/10.1002/art.10696>.
  33. Strieter RM, Keeley EC, Hughes MA, Burdick MD, Mehrad B. The role of circulating mesenchymal progenitor cells (fibrocytes) in the pathogenesis of pulmonary fibrosis. *Journal of Leukocyte Biology*. 2009;86(5):1111-8, <http://dx.doi.org/10.1189/jlb.0309132>.
  34. Pilling D, Fan T, Huang D, Kaul B, Gomer RH. Identification of Markers that Distinguish Monocyte-Derived Fibrocytes from Monocytes, Macrophages, and Fibroblasts. *PLoS ONE*. 2009;4(10):e7475, <http://dx.doi.org/10.1371/journal.pone.0007475>.
  35. Freshney RI. *Culture of Animal Cells: A Manual of Basic Technique and Specialized Applications*. 6th ed. Hoboken: John Wiley & Sons, Inc.; 2010.
  36. Weatherford HL. Chondriosomal changes in connective-tissue cells in the initial stages of acute inflammation. *Cell and Tissue Research*. 1933;17(3):518-41.